Mechanisms of physical stabilization of concentrated Water-in-Oil emulsions probed by Pulse Field Gradient Nuclear Magnetic Resonance (PFG-NMR) and rheology through a multi-scale approach.

Diego Pradilla[a], Ana Barrera[a], May Grete Sætran[b], Geir Sørland[b], Oscar Alvarez[a].*

[a]Grupo de Diseño de Producto y de Proceso (GDPP), Departamento de Ingeniería Química, Universidad de los Andes, Carrera 1 este No. 18A-12, Edificio Mario Laserna, Piso 7, Bogotá, Colombia.

[b]Ugelstad Laboratory, Department of Chemical Engineering, The Norwegian University of Science and Technology (NTNU), Trondheim, Norway.

*Corresponding Author

E-mail: d-pradil@uniandes.edu.co

Phone: (+57)-1-3394949 ext. 3095

Conflict of interest disclosure

The authors declare no competing financial interest.

Keywords: PFG-NMR, Multi-scale approach; Rheology, Inverse emulsions

ABSTRACT

The long-term physical stability of surfactant-stabilized (Span80® and Tween20®) concentrated water-in-mineral oil (W/O) emulsions in the presence of an electrolyte (NaCl) was studied. Pulse field gradient NMR and rheology (bulk and interfacial) were used to probe the response at the macroscopic, microscopic and molecular levels rendering a multi-scale approach. Results show that: i) emulsions prepared with NaCl exhibit higher values of the elastic shear modulus ($G'_{with\ NaCl} > G'_{without\ NaCl}$) even after ~20 days, ii) the stabilization effect of salt against coarsening of droplets is not due to differences in droplet size (and thus G') or the energy incorporated through emulsification and iii) NaCl relaxes the liquid-liquid interface via a salting-in effect which results in a lower interfacial shear elasticity ($G^{s\prime}_{with\ NaCl} < G^{s\prime}_{without\ NaCl}$) but a higher resistance to coarsening events due to changes in the adsorption density of the layer.

INTRODUCTION

Emulsions are a type of colloidal system[1] that are found at different industries: cosmetics, in the form of moisturizing creams, lotions and other personal care items[2]; food, in the form of flavored beverages, dairy-based products and sauces[3]; pharmaceuticals, where the active ingredients are trapped inside the droplets for delivery once ingested[4]; and they are undesirably found in the petrochemical industry where the indigenous components of oil such as the asphaltenes, resins and naphthenic acids stabilize these systems forming a solid-like interface that hinders coalescence and retards film drainage[5-7]. Emulsions (i.e. macroemulsions) are thermodynamically unstable dispersions of two immiscible liquids in the form of droplets that require an external source of energy to overcome their non-

spontaneous formation nature[8-9]. This energy can be mechanically supplied by means of a mixing device through the emulsification process. This, coupled with the action of a surfactant that adsorbs at the liquid-liquid interface, lowers the interfacial tension, forms an interfacial film and ensures a short range repulsive interaction, stabilizes the system against phase separation[10].

Polydisperse highly concentrated or high internal phase ratio emulsions are a subject of particular interest in all the above mentioned areas of industrial application because of their complex rheological behavior which is due to the increase in droplet-droplet interactions as they go above the limit of the closest packing[10-11]. In this region, droplet networks are formed and their spherical shape is lost resulting in irregular polyhedrons (Fig. 1). This transition also results in non-Newtonian behavior which in this case can be characterized by two aspects: the typical drop in viscosity as the shear rate increases[12-13] and the appearance of a yield stress characterized by the absence of flow at certain shear stresses[12, 14]. Additionally, the viscoelastic behavior is characterized by first, the independence of the elastic modulus in a wide frequency range (and vice-versa, the independence of the elastic modulus in a wide oscillatory stress range), second the increase of the elastic and loss moduli as a function of both the droplet size and the energy incorporated through the emulsification process. And third, the non-linearity of the visco-elastic properties at high deformations (or high oscillatory stresses) that lead to a type of softening of the material, sometimes interpreted as a mechanical glass transition[15-18].

The physical stability of surfactant-stabilized highly concentrated emulsions usually refers to the different events that take place at the liquid-liquid interface and ultimately lead to phase separation. The timeframe of these phenomena is wide and can vary from minutes to the

order of years depending on the industrial application[19]. The long term physical stability of emulsions has been traditionally explained through five mechanisms, namely, creaming/sedimentation, flocculation, coalescence, Ostwald ripening and phase inversion[19]. Evaporation of the aqueous phase has also been presented as a possible mechanism[20].

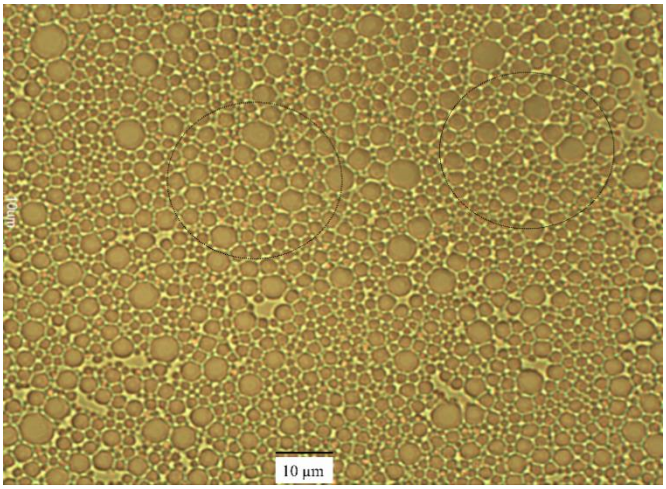

Figure 1. Optical micrograph of a highly concentrated water-in-mineral oil emulsion showing non-spherical droplets (circled areas) of less than 5 µm. The volume fraction in this case is 88%.

Physical stability is affected by several variables: droplet size, polydispersity, concentration of the dispersed phase, solubility, the chemical nature of the surfactants and the presence of other species that are not necessarily surface active such as short-chain alcohols and inorganic salts (e.g. NaCl, KCl)[21]. Inorganic electrolytes and their role in emulsion stability is of significant relevance because a considerable amount of products contain them: drilling and injection fluids for the oil industry, personal care products such as sunscreens, eye liners, hand lotions, liquid soaps, shampoos and a vast amount of food products such as vinaigrettes, ketchup, mayonnaise, yogurt, fruit juices, etc[22-23]. In a study[24], the presence of $MgSO_4$ in benzene-in-water emulsions showed that the extended electrical double-layer decreased the energetic barrier to flocculation for concentrated emulsions despite a significant surface potential. A study[25] on surfactant-stabilized highly concentrated water-in-oil emulsions in

the presence of $MgSO_4$ demonstrated that coalescence was significantly reduced due to the greater surface excess concentration of various surfactants of varying Griffin's hydrophilic-lipophilic balance HLB[26]. Regarding interfacial properties, it has been suggested[27] that the addition of NaCl to water-in-mineral oil emulsions decreases the interfacial elasticity (i.e. the interfacial elastic modulus $G^{s\prime}$) during the stages of diffusion-controlled adsorption of different surfactants due to a salting-out effect. Similar to the case of polymers and particles, it has been suggested[28] that the stability of water-in-oil emulsions can be described through depletion flocculation theory, however the presence of other high-molecular weight additives in the aqueous phase is imperative, otherwise osmotic pressure would not be developed. Even though the stability of water-in-oil (W/O) emulsions cannot be explained through the traditional DLVO theory due to the low dielectric constant of the continuous phase, electrostatic effects should not be ruled out, especially in the case of W/O emulsions stabilized with non-ionic surfactants which could develop charge as a result of ionic impurities[22, 29-30].

Among the most traditional tools for assessing the long-term physical stability of emulsions is rheology. It has been previously stated[31] that the evolution of the viscosity with time is strongly related to the changes in average droplet size and so a decrease in the dynamic viscosity correlates to an increase in the average droplet size and in some cases it follows first-order kinetics[19]. The shear elastic modulus (G') can be used to assess the extent of a flocculated structure in an emulsion through a correlation with the cohesive energy. In general terms, for diluted emulsions, when G' increases rapidly in the low-frequency region outside the linear viscoelastic area, the stronger the flocculation[32]. Flow curves (shear stress vs shear rate) can also be used to assess the degree of thixotropy or sol-gel transitions. In this

case the degree flocculation, creaming or sedimentation can be evaluated. Light and dynamic light scattering (LS/DLS) and the dynamic dispersion of light (DDL) are other useful techniques that are traditionally used to study physical stability phenomena such as Ostwald ripening and coalescence[7, 33-34]. Finally, in the specific case of petroleum emulsions, an invaluable tool for assessing the stability of emulsions and the efficiency of emulsion breakers is bottle testing. Even though this is a semi-quantitative approach, it provides intuitive information about the physical stability of these complex systems[35-36].

Traditionally, Nuclear Magnetic Resonance (NMR) has been a tool used in medical applications for imaging and disease detection. However, as early as 1968 pulse-field NMR protocols were already in place for determining average droplet size and droplet size distributions[37]. Two main drawbacks that lasted over 20 years with this methodology made it unsuitable for different studies: first, before measurements a droplet size distribution (e.g. log-normal) had to be assumed for post-data fitting; and second the impossibility of removing the signal generated by the oil phase which made following the water phase difficult. During the late 1990's protocols and sequences were adjusted to determine pore and particle size of different systems (e.g. cosmetic, food, petrochemical emulsions) through self-diffusion[38-39] but it was not until recent advances and breakthroughs[40] that new protocols and sequences were developed to overcome the above mentioned problems providing a novel methodology for true average droplet size and droplet size distributions An additional advantage of NMR instruments, particularly the one used in this work, is that it can actually be used as an on-the-bench device since its size is not significantly bigger than a desktop computer. This would allow faster online routine measurements with more accuracy and precision.

In summary, the theory behind droplet size determination through NMR sequences is as follows: Mitra et al[41]. showed that the initial time dependency of the restricted diffusion coefficient of water confined in a droplet can be written as follows (Eq.1):

$$\frac{D(t)}{D_0} \approx 1 - \frac{4(D_0 t)^{1/2}}{9\sqrt{\pi}} \frac{\bar{S}}{V} \qquad (Eq.1)$$

Where $D(t)$ is the time dependent apparent restricted diffusion coefficient, D_0 is the unrestricted diffusion coefficient in the bulk fluid, t is the observation time and $\bar{S}/V$ is the average value for the surface to volume ratio. In an emulsion, a wide range of droplet sizes can be present, which can be reflected from the so-called transverse relaxation time (T_2) experiment that results in an actual and true droplet size distribution. This is achieved through pulses of a given strength, hence the name Pulse Field Gradient (PFG). The pulses are oriented and modified according to a fixed sequence that follows how water is distributed in the sample, suppresses the oil phase signal and quantifies and extracts a droplet size distribution without assumptions on the shape. A more detailed explanation on the extraction of droplet size distributions from pulses in NMR can be found elsewhere[39-41].

In this study, a multi-scale approach[42-43] is used for the analysis and evaluation of the effect of electrolytes (i.e. NaCl) on the short and long-term physical stability of surfactant-stabilized water-in-mineral oil model emulsions with the incorporation of Pulse Field Gradient NMR as a modern and reliable tool for following phase separation[44]. Three different scales are coupled and analyzed transversally: molecular through the measurement of the interfacial elasticity, microscopic through the determination of the average droplet size and macroscopic through the quantification of the energy incorporated during the emulsification process and the determination of the elastic modulus (G').

MATERIALS AND EXPERIMENTS

Materials. Highly concentrated inverse (water-in-oil) emulsions were prepared with mineral oil (USP-grade, density 850 kg/m^3 at 25℃, dynamic viscosity ~0.2 $Pa \cdot s$ at 20℃), type 2 mili-Q de-ionized water and two non-ionic surfactants provided by Croda: Sorbitan Monooleate (Span 80®), oil soluble with a hydrophilic-lipophilic balance (HLB) of 4.3, and polisorbate 20 (Tween 20®), water soluble and HLB=16.7. The mass ratio of Tween 20® to Span 80® was kept at 78:5 to ensure maximum physical stability during the timeframe of the experiments (approximately 4 hours) thus achieving a homogeneous sample (e.g. droplet size, elastic modulus) in all experiments. The electrolyte chosen for this work was sodium chloride Emsure® (NaCl) purchased from Sigma-Aldrich and the concentration was kept constant for all emulsions at 0.5 %wt. The total amount of emulsion prepared for all cases was 250g.

Emulsification process. This process consisted of three steps that were carried out at a constant temperature of 25°C to avoid undesired temperature effects.

Continuous and dispersed phase pre-homogenization. Tween 20® (and NaCl for emulsions with salt) was pre-mixed with the aqueous phase (water). Separately and simultaneously Span 80® was pre-mixed with oil. This process was carried out with a propeller-type of impeller at 300 RPM using a Hei-Torque Precision 400 mixer (IKA Instruments). The total amount of surfactant was 1.5 %wt and the ratio of the two surfactants was set to achieve a global HLB of 5. In order to establish an adequate baseline for measurements within the experimental window (30 minutes after preparation), stability tests with a Turbiscan® Lab analyzer (Formulaction, France) were performed at different surfactant concentrations (i.e.

varying the total amount) and 1.5 %wt was the concentration that at which destabilization mechanisms that lead to phase separation in the short-time did not take place.

Incorporation of the dispersed phase. The aqueous phase was incorporated into the oil phase at a rate of 0.5 mL/s using a Fischer Scientifics peristaltic pump. A propeller-type of impeller was used with a tip speed of 1.7 m/s in a system where the impeller-to-tank diameter ratio was 0.78.

Final homogenization. After incorporation of the dispersed phase, emulsions were homogenized for 10 minutes at the same conditions of the incorporation step ensuring a constant torque which represents a consolidation of the different processes taking place. Parallel experimentation at various times (up to 40 minutes) showed that for these systems, this step does not significantly change the final properties of the emulsions (data not shown). This results is expected given that the kinetic stability of such emulsions, from an industrial perspective, must be high so that the sensory perception of the consumer is not influenced.

Emulsions were prepared within a volume fraction range of 56 % and 88 % with increments of 10 %. Unless otherwise specified, reproducibility was ensured by performing all measurements by triplicate. Results correspond to the average of all tests. All the emulsions were characterized 5 minutes after the final homogenization step and time-dependent values obtained at the stated timeframe.

Molecular scale: interfacial elastic modulus ($G^{s\prime}$).

Interfacial shear rheology. A double wall-ring (DWR) geometry was used to measure the shear interfacial elastic modulus ($G^{s\prime}$). In this setup, the ring made of Pt/Ir is positioned at the liquid-liquid interface and the sample contained in a trough made of Delrin®. The ring

and the trough were thoroughly cleaned before and after each experiment to prevent the undesired adsorption of impurities. The rest of the setup is extensively explained elsewhere[45]. The aqueous phase (water, surfactant and salt) is carefully poured onto the trough with the help of a micropipette (18.5 mL). The ring is then placed at the interface. Finally, the oil phase (mineral oil and surfactant) is carefully placed on top with the help of a micropipette (5 mL). The amounts of each phase, surfactant and salt placed on the rheometer are equivalent to the amounts used to form the emulsions.

The value of the shear interfacial elastic modulus was calculated through oscillatory tests in the linear viscoelastic region. The first test was an interfacial stress sweep from 10^{-4} to $10^{-1}\ N/m$ at a constant frequency of $10^{-1}\ rad/s$. The second test was an oscillatory frequency sweep from 10^{-3} to $10\ rad/s$ at a constant stress of $10^{-5}\ N/m$. All experiments were performed at 25°C and the results reported correspond to the average value of duplicates.

Microscopic scale: average droplet size and Pulse Field Gradient NMR.

Two different techniques were used to measure and determine average droplet sizes and droplet size distributions: Pulse Field Gradient NMR (PFG-NMR) and Light Scattering (LS).

Pulse Field Gradient NMR (PFG-NMR).

An advanced and portable 0.5 Tesla NMR spectrometer (Anvendt Teknologi AS) equipped with a 300 W RF transmitter and permanent magnets with 20 MHz resonance frequency, H_1^+ probe with 1-dimensional gradient coils capable of delivering pulses of 350 G/cm mounted on pole pieces was used to probe the emulsions in a 20 mm-height and 18 mm-diameter sampling tube. The strength of the pulses is suitable for systems in which the diffusion

coefficient is as low as $\sim 10^{-13}\ m^2/s$ and the temperature is thoroughly controlled through air flow.

The sample tube is placed inside the instrument and then the pulse-protocol is activated. The process to obtain average droplet size and droplet size distribution through NMR pulses takes less than 1 minute and is described next. The pulse sequences (or protocol) used for determining the droplet size of emulsions are constructed in four sections and visually represented in Fig. 2. i) magnetization is spoiled by two 90° RF pulses simultaneously with a set of bipolar gradients (GS1 and GS2 in Fig. 2) of different duration and strength[40]. The magnetization takes some time to recover and this is called the spoiler recovery delay (SRD). When the SRD is shorter than T_1 (the longitudinal relaxation time or the time back to thermal equilibrium) by a given factor (e.g. 5 times in this case) rapid data acquisition is possible. ii) suppression of the signal corresponding to the continuous phase of the emulsion is achieved[44] through 1 loop of the 13-interval pulse field gradient stimulated echo (PFGSE) sequence shown in Fig. 2 as the main sequence. The parameters $g, f\ and\ \Delta_i$ are chosen depending on whether differences in relaxation or restricted diffusion are applied for signal suppression. The sections i) and ii) just described are called the Spoiler Recovery (SR) one-shot sequence because the two data points required for water quantification are recorded in one step rather than performing two different measurements with different Δ_i values. Section iii) is related to the part of the sequence that is used to extract the droplet sizes once the signal of the continuous phase has been suppressed. An 11-interval pulse field gradient spin echo (PFGSE) (Fig. 2 route A)[46] was used and a z-storage delay (Δ_2) included to minimize unwanted noise from any residual eddy current transients that might arise after sections i) and ii). And iv) the T_2-relaxation is recorded using the SR one-shot sequence followed by a

Carr-Purcell-Meiboom-Gill (CPMG) sequence (Fig. 2 route B). The results of applying the sequences presented in Fig. 2 are a droplet size distribution and an average value for the droplet size (Fig. 8 of the text and Figure S4 of the supplementary material show measured values and ranges obtained for the emulsions prepared in this work). More details of the experimental setup and validity of the sequences can be found elsewhere[40, 44].

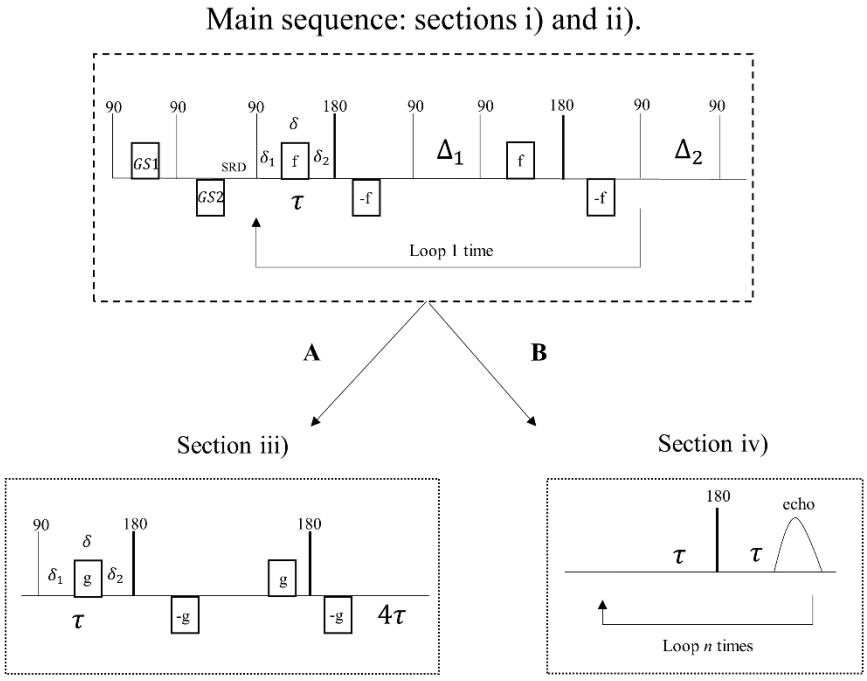

Figure 2. Sequences used in PFG-NMR to determine droplet size and droplet size distributions. Sections i and ii are used for signal suppression; section iii (route A) for average droplet size and section iv (Route B) for droplet size distribution.

Light Scattering (LS).

The droplet size distribution was obtained using a Mastersizer 3000 (Malvern Instruments), which uses the laser diffraction technique to perform droplet size measurements in the range from 0.01 to 3500 μm. The governing principle for these measurements is the Mie theory. To avoid multiple scattering, adequate ranges of obscuration were selected according to the laser specifications. All measurements were performed under the same conditions.

Mie theory considers the diffraction, refraction and absorption events that occur when a beam of light impacts a particle. For this reason, the optical parameters must be known. The dispersant, which carries the particles or droplets to the measurement area, must not interact in any way with the droplets to avoid changes in size; for this reason, mineral oil was the dispersant chosen.

From the intensity reports, which are related to the volume that the particles occupy, various mean diameters can be obtained. One of these is the volume mean diameter, D[4,3] or De Brouckere diameter which is the mean diameter reported in this work.

Macroscopic scale: energy and elastic modulus G'.

Quantification of the total energy incorporated. In order to quantify the total energy incorporated through the emulsification process (pre-homogenization, incorporation and final homogenization steps) the following procedure was used based on the torque vs time data obtained from the mixing unit. First, the power (J/s) was calculated by multiplying the torque and the angular velocity. Second, numerical integration of the power vs time data was performed. This integration yields units of energy (J). Finally, to normalize and compare the energy applied to different emulsions of different concentrations (hence different energy),

the total amount of energy (J) was divided by the final volume of the emulsion to get units of energy per volume of emulsion (J/mL).

Elastic modulus (G'). A controlled-stress rheometer (ARG2, TA instruments) equipped with a 20 mm-parallel plate geometry was used to perform 2 oscillatory tests at a constant gap of 1 mm and constant temperature of 25°C with a maximum deviation of ± 0.1°C. An extra set of oscillatory tests was carried out varying the gap size (500-1500 μm) to ensure that there was no wall-slip. These results were not included in the analysis.

The first oscillatory test was a frequency sweep with a pre-shear of 1 minute at 1 s^{-1}, followed by the frequency step of 0.1 to 100 rad/s at a constant oscillatory stress of 2 Pa. The second oscillatory test was a stress sweep with a pre-shear of 1 minute at 1 s^{-1}, followed by the stress step of 0.01 to 100 Pa at a constant oscillatory frequency of 5 rad/s. These tests allowed for the calculation of the elastic modulus (G') in the linear viscoelastic region. In this case, it means that G' is independent of both the stress and the frequency, thus the value reported corresponds to the average in the plateau region. No creaming or other signs of instability were observed during the experiments. Additionally, it is important to mention that the linear viscoelastic region also holds when the strain sweeps at the probed stresses and frequencies were performed (data not shown).

Due to the liquid-like nature of the emulsions at a volume fraction of 56 % of dispersed phase, the oscillatory tests were carried out in a concentric cylinder-geometry with a constant gap of 5920 μm. All the other conditions remained the same.

RESULTS AND DISCUSSION

The effect of NaCl on the elastic modulus (G') and average droplet size ($D[4,3]$).

The elastic modulus in the linear viscoelastic region (i.e. low frequency plateau values) as a function of the volume fraction of the dispersed phase for the W/O emulsions prepared with and without NaCl is plotted in Fig 3. First, an increase of G' with φ for both emulsions is observed. This result is consistent with the literature[16, 47] and this behavior is normally attributed to a decrease in droplet size that potentiates droplet-droplet interactions due to packing of the disrupted droplet network when it transitions from diluted to highly concentrated emulsions. This is also consistent with the results of Lacasse et al.[48] Who explain the increase in the static elastic shear modulus through an energetic effect of the compressed droplets that turn to flattened facets capable of storing energy. In polydisperse systems the effects are more pronounced because droplets of various sizes and hence different Laplace pressures act differently on each other to maintain mechanical equilibrium. In this case (Fig. 4) droplet size remains essentially constant because the emulsions of this work belong to the highly concentrated regime. Second, even though the trend is the same, emulsions prepared with NaCl show higher values of G' than emulsions without salt. It has been previously reported that addition of electrolytes increases the stability of emulsions[49]. Among the reasons for this are first, the interaction with surfactants by varying the spontaneous curvature thus bending the adsorbed layer towards water (in the case of nonionic surfactants); second, electrolytes and surfactants tend to form non-relaxing rigid films that hinder coalescence[50] with the additional effect in which salts decrease the strength of attractive forces (Van der Waals)[51-52]; and finally adsorption effects in which electrolytes and surfactants co-adsorb reducing the interfacial tension and promote the interactions at the liquid-liquid interface of the adsorbed layer by modifying the ionic strength of the medium. The electrolyte can also act as a bridge between the polar head of the surfactant providing a more evenly distributed surface coverage of the droplet[52]. Thus the macroscopic effect of

adding salt to W/O emulsions is represented by an increase in G' which would normally be translated as a system with higher elasticity.

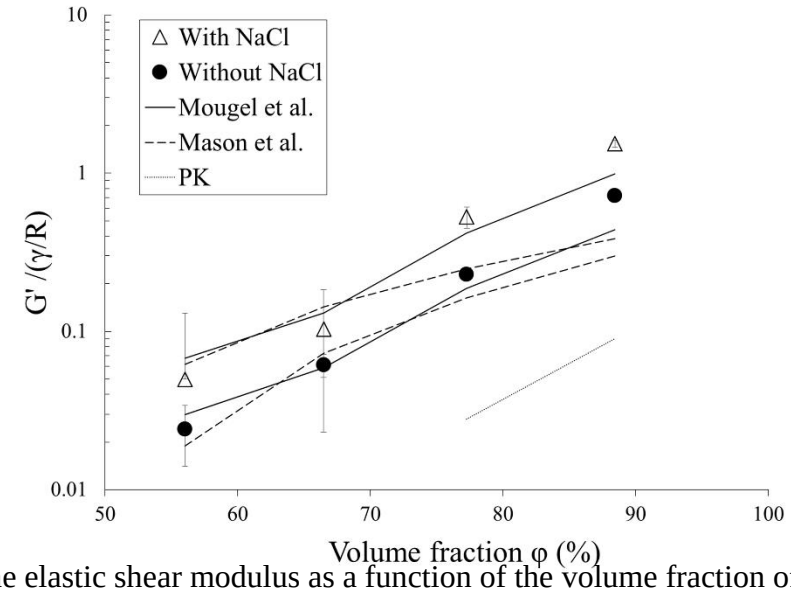

Figure 3. The elastic shear modulus as a function of the volume fraction of the dispersed phase for emulsions prepared with 0.5 %wt of NaCl (empty symbols) and without NaCl (filled symbols). The fit to the Princen and Kiss (PK) model, the Mason et al. model (with: $\varphi^* = 0.64$) and the Mougel et al. model (with: $A_{with\ NaCl} = 0.43$, $A_{without\ NaCl} = 0.18$ $\varphi_c = 0.96$ and $D_0 = 30\ nm$) are also shown. .

Fig. 3 also shows the fit of the elastic modulus to three different models: Princen and Kiss[53] (PK), Eq. 2,Mougel et al.[54], Eq. 3 and Mason et al[55]., Eq. 4

$$G' = 1.769\ \frac{\gamma}{R_{32}}\varphi^{1/3}(\varphi - 0.712) \qquad (Eq.2)$$

$$G' = \frac{2\pi\gamma A D_0 \varphi}{R^2(\varphi_c - \varphi)} \qquad (Eq.3)$$

$$G'/(\gamma/R) = \varphi^2(\varphi - \varphi^*) \qquad (Eq.4)$$

The parameters of Eq. 2 are: γ is the interfacial tension and R_{32} is the Sauter mean radius. Given the high amount of surfactant used in all emulsions (1.5 %wt.) the interfacial tension (at equilibrium) remains constant ($\gamma = 4.3\ mN/m$) for emulsions of varying volume fraction

of the dispersed phase. It is different in value ($\gamma = 3.8\, mN/m$) but also constant when salt is added. This was corroborated through interfacial tension measurements (data not shown).

The parameters of Eq. 3 are: γ is the interfacial tension, R is the average droplet radius that can be obtained from the $D[4,3]$ mean diameter, A is a fitting parameter specific to the system in question and D_0 is the intermolecular distance between droplets[56] and φ_c is the critical volume fraction[54]. For the case of the emulsion in this work: $A_{with\ NaCl} = 0.43$, $A_{without\ NaCl} = 0.18$ $\varphi_c = 0.96$ and $D_0 = 30\ nm$.

The parameters of Eq. 4 are: γ is the interfacial tension, R is the average droplet radius that can be obtained from the $D[4,3]$ mean diameter and φ^* is the random close packing fraction. In this case, this value was taken as 0.64, that is, the highest volume fraction at which disordered monodisperse spheres can be packed. This value is not expected to vary significantly when disordered polydisperse systems are used[55].

Princen and Kiss[53] stated that the constants associated to their model slightly depend on droplet size distribution and the thickness of the thin films and so as the model approaches the limiting value of $\varphi \sim 1$ the elastic modulus would be overpredicted by a factor of 2. Pal[13] further explored the applicability of the PK model as well as a modification that included a strong dependence of G' with the thickness of the thin films. In both cases, the shear elastic modulus was underpredicted. This overall underprediction of the shear elastic modulus is not due to the effect of film thickness, but instead, as shown by Mougel et al.[54] deviation from the PK model for emulsions above φ_c arises because of the preponderance of van der Waals interactions when droplets and deformed droplets are in constant contact. This strong interaction is represented by the amplitude of the van der Waals energy ($W = \frac{A_H R}{12D}$) that

depends on the Hamaker constant demonstrated by Israelachvili[51] and included in the Mougel et al. model. This scenario not only correctly predicts the behavior of the shear elastic modulus in the highly concentrated range but also includes an energetic explanation when droplet deformation is present.

Fitting the data of this work to the PK model clearly yields the expected underprediction of the shear elastic modulus (G') in all cases (the PK model was only applied for volume fractions higher than 0.712, otherwise $G' = 0$). The validity of the PK model has been discussed and argued against mainly because it does not consider the effect of the transition zone that arises when systems above the maximum packing volume fraction inherently cause the droplets to undergo deformation and the thin films are in permanent contact[13, 54, 57]. The PK model also under-predicts the elastic modulus even when the effect of the film thickness is mathematically removed, which suggests that the parameters of the model are not universal but instead system-specific[57]. Princen and Kiss extrapolated the model originally developed for foams to an O/W emulsion prepared with an anionic surfactant, something that definitely causes changes in the fitting parameters.

Analogously, the Mougel et al. model, which was tested on a water-in-mineral oil stabilized by a non-ionic surfactant (besides another system reported in the literature), shows a good correlation with the data because of the preponderance of the van der Waals forces when thin films are in close contact that scales better with an R^{-2} dependence, a non-linear variation of the effective volume fraction and an upper limit for emulsification, or divergence, determined by the parameter (φ_c). It is important to highlight that the Mougel et al. model is also valid for emulsions prepared with NaCl, which suggests that a quantification of the extent of the

Hamaker constant (represented partly by the fitting parameter A) is possible in the presence of an electrolyte.

The PK model is a two-dimensional model in the sense that droplets are actually treated as circles (i.e. the surface of the droplet or perimeter is parametrized by one radius of curvature) which tends to ignore the anharmonic response of polydisperse emulsions under deformation. In contrast, the Mason et al. model is a 3D model which accounts not only for harmonicity but also incorporates an interdroplet potential of repulsive origin providing a more realistic estimation of the elastic shear modulus and the osmotic pressure. In fact, Mason et al. showed that for emulsions in the highly concentrated regime, ($\varphi > \varphi^*$) the magnitude of the normalized osmotic pressure and elastic shear modulus are similar. This result also shows that the 3D model accounts for the crossover from entropically dominated regime (dilute regime) to the interfacially dominated regime as $\varphi \sim 1$.[55, 58] The graphical result of these remarks predicts three regions: first, a saddle point-like transition at the vicinities of the maximum packing fraction ($\varphi \approx \varphi^*$). In this region, the elastic shear modulus increases monotonically; second, an attenuated increase of the shear elastic modulus ($\varphi > \varphi^*$) that tends to plateau. And third, the region where $\varphi \sim 1$ which shows an even smoother increase of the elastic modulus. In this area, just as the authors point out, a small underprediction of the modulus occurs because experimental data normally shows a sharp increase that could be asymptotic. Not surprisingly the 2D Mougel et al. model also captures these effects due to the incorporation of the Van der Waals interaction parameter. Fig. 3 shows excellent agreement with the predictions and considerations of the models reproducing the mentioned areas.

An interesting aspect of these W/O emulsions is that their average droplet size remains virtually unchanged when NaCl is added (taken into account the error bars). Fig. 4 shows a plot of the average droplet size D[4,3] measured through LS as a function of the volume fraction of the dispersed phase φ after preparation. This suggests that the short-term physical stability of these emulsions correlates with the rheological results of Fig. 3 in the sense that the higher elasticity achieved with the addition of salt is not due to changes in droplet size caused by coarsening but instead to molecular aspects such as electrolyte co-adsorption and bridging[25] that will be described in a later section. In fact, Fig. 5 shows a plot of the evolution of the elastic modulus with time and it can be observed that G' remains consistently higher for emulsions prepared with salt after 20 days of analysis. Additionally, Fig. 5 shows that G' tends to decrease with time for all emulsions. This is expected not only because of an increase in the average droplet size (Fig. 6) but also because the coarsening process responsible for droplet size changes reduces the preponderance of van der Waals interactions as the droplets are no longer in constant contact.

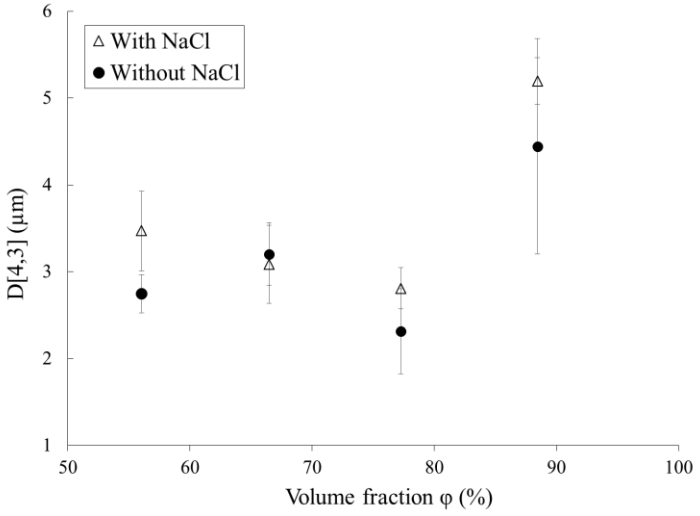

Figure 4. Average droplet size measured through LS as function of the volume fraction of the dispersed phase φ for emulsions prepared with 0.5 %wt of NaCl (empty symbols) and without NaCl (filled symbols).

This suggests that the mechanisms involved at the molecular level (interactions at the liquid-liquid interface) that produce a microscopic response (droplet size) are consistent with the macroscopic response of the system through the elastic modulus. Fig. 5 also suggests, as it will be seen in the next section, that coarsening of water droplets occurs, most likely through Ostwald ripening[25] rather than coalescence, but the electrolytes delay this process. Fig. 6 shows a plot of the evolution of the average droplet size during the 20-day experimental window where the changes reported correlate with the changes in rheology. Even though LS is a powerful tool for determining average droplet size and distributions, it has some inherent flaws (such as the need of dilution prior to measurements, tuning of optical parameters and mathematical adjustment of distributions) that can be overcome by using different methods such as PFG-NMR as it will be shown in the next section.

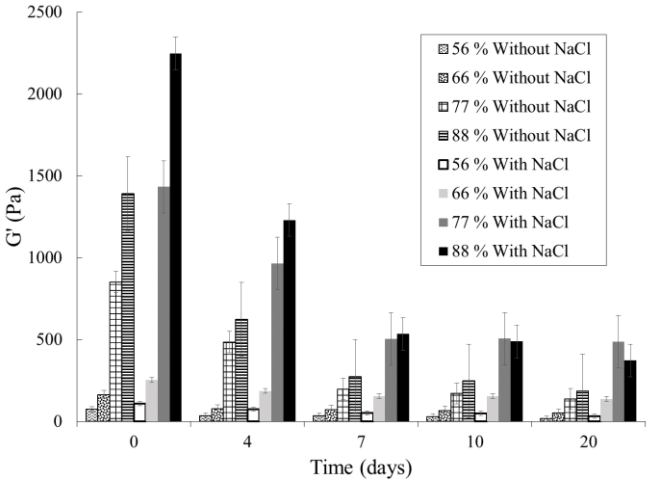

Figure 5. The elastic shear modulus as a function of time for emulsions prepared with and without NaCl within the concentration range used in this work.

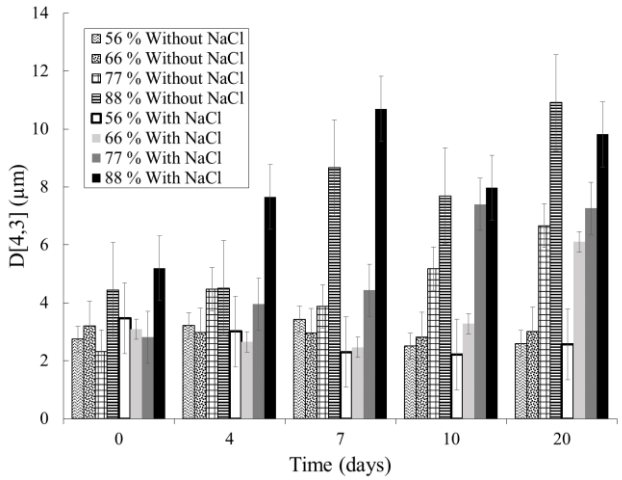

Figure 6. Average droplet size as function of time for emulsions prepared with and without NaCl within the volume fraction of dispersed phase range used in this work.

Droplet size, droplet size distribution and PFG-NMR.

In this work, special attention was given to W/O emulsions prepared in the highly concentrated regime, that is, volume fractions of 77 and 88 % because in this region, the interactions that take place at the liquid-liquid interface tend to be more pronounced (i.e. van der Waals forces have a stronger influence when the droplet thin films are in close, constant contact). The time-dependent droplet size distributions for these emulsions at 25°C are shown in Fig. 7. It can be seen that the droplet size distributions (DSD) of emulsions prepared with NaCl (Fig. 7a and Fig. 7c) do not change either in shape or intensity. For the emulsions prepared without NaCl (Fig. 7b and Fig. 7d) the situation is clearly different as there is both a shift of the DSD towards larger droplets and a loss of intensity (frequency). The shift towards larger droplets is most likely due to coarsening of the droplets while the intensity loss is a manifestation of evaporation of small portions of water from the bottom of the sample. The area under a distribution curve is proportional to the water content of the emulsion. The corresponding average droplet sizes at 25°C are presented in Fig. S1 of the supplementary material and it is important to highlight that the results correlate reasonably well with the LS calculated average droplet size even though there are some inherent flaws of the technique that are not expressed in PFG-NMR measurements.

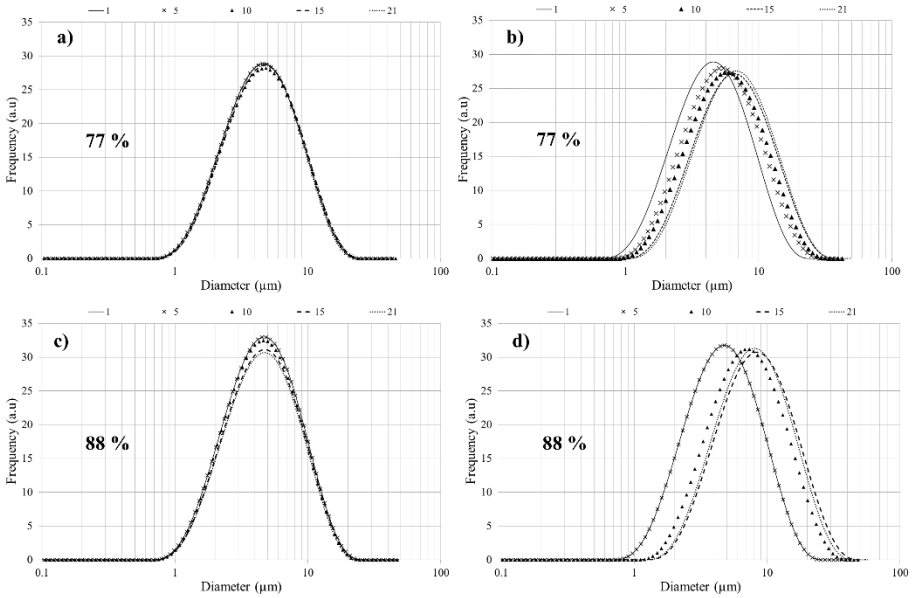

Figure 7. Droplet size distributions measured through PFG-NMR for emulsions prepared with 0.5 %wt of NaCl (a,c), without NaCl (b,d) at volume fractions of the dispersed phase of 77 and 88 % and their evolution for 21 days at 25°C.

The average droplet size for emulsions prepared with NaCl measured through LS (Fig. 6) and measured through PFG-NMR (Fig. 7) apparently show different results. While LS shows an increase of the average droplet size, PFG-NMTR does not. As previously stated this is due to the limitations of LS as a technique when the sample must be diluted before measurement. This situation changes the conformation of the droplet-network, especially in a highly

concentrated system where deformation is present. Additionally, LS gives data points for the average droplet size presupposing a distribution (Mie theory) and then fitting the results to that distribution while PFG-NMR shows the actual and true distribution of the water phase inside the sample. From Fig. 6 and Fig. S1, it can be clearly seen that both values are within the same order of magnitude ($D[4,3] at\ 0-24\ days \sim 4-8\ \mu m$, average droplet size through PFG-NMR $at\ 0-24\ days \sim 5-6 \mu m$), something that a technique such as LS cannot distinguish, which explains the apparent discrepancy in the values.

It was previously mentioned that the mechanism behind coarsening of the droplets for these highly concentrated systems is most likely Ostwald ripening. Fig. 8 (and Fig. S2 of the supplementary material) show the evolution of the cube of the radius (R^3) and the average droplet size as a function of time for all the emulsions of this work analyzed with PFG-NMR. According to Weis et al.[59] when the dominating mass transfer mechanism is the diffusion of molecules between the droplets, the increase in droplet radius with time should be proportional to the cube of the initial droplet radius. As seen in Fig. 8 the fit to a linear equation is consistent with these remarks. Evidently, this is valid for emulsions prepared without the addition of NaCl given that emulsions in the presence of an electrolyte show little to no signs of destabilization during the experimental window. Additionally, the steady and monotonic increase of the average droplet size with time for emulsions prepared without NaCl and the absence of a transition zone (i.e. asymptotic regime) is another indication of a diffusion-controlled ripening[60-61]. Moreover, given that that the evolution of the average droplet size with time for emulsions in the presence of an electrolyte is virtually negligible, if coarsening is present to some small extent, it would be through coalescence rather than Ostwald ripening because of the almost negligible increase with time[60]. This is also consistent

with previous remarks where it was suggested that mass transfer across the droplets in such concentrated systems is due to the direct contact of the thin films where reversible hole-nucleation occurs thus allowing mass transport between droplets[60, 62].

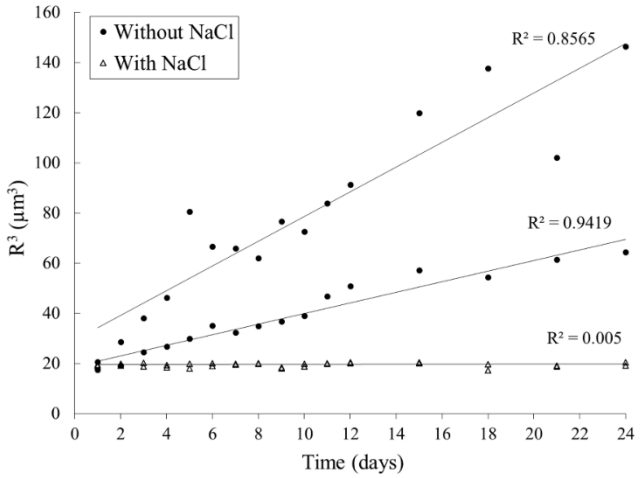

Figure 8. Variation of the radius with time calculated using PFG-NMR for emulsions with a volume fraction of the dispersed phase of 77 and 88 % at 25°C in the presence of NaCl and without. The solid lines represent a linear fit to test for Ostwald ripening.

These results confirm the hypotheses and remarks of the previous section: a) the initial droplet size for emulsions with and without salt is similar, b) emulsions prepared with NaCl remain stable for 20 days with low variations in droplet size and c) emulsions without the presence of electrolytes are more unstable evidenced through the shift of the distributions to areas of larger droplet size due most likely to Ostwald ripening. These observations remain

true when the temperature is increased to 50°C and the destabilization is more evident (Fig. S3 and Fig. S4 of the supplementary material).

Thus far the link between the response of the system at the macroscopic (G') and microscopic levels (droplet size) has been evaluated. However, an important parameter that is essential for an adequate multi-scale approach[42-43] assessment is the energy incorporated through the emulsification process (E_v). This parameter is of importance because a fixed composition-concentration emulsion can have a wide range of droplet sizes. Hence to avoid the effects associated to a mechanical mixing process, an analysis over the energy was performed. Fig. 9 shows a plot of the elastic modulus as a function of the energy incorporated. From this figure it can be observed that in general terms, the emulsions prepared with NaCl consistently required less energy to produce a system with similar droplet size and higher G'. This behavior, which is non-intuitive for emulsions where droplet size and droplet size distributions are similar, could be attributed to the different processes that take place at the liquid-liquid interface. In this case, a favorable energetic state is generated when the salt within the aqueous phase dissociates and interacts with the polar heads of the surfactants. A type of bridging occurs and this changes the adsorption density of the surfactants at the interface relaxing it. Additionally, when the salt dissociates, it could interact with surface active impurities from the mineral oil and surfactants and this interaction reduces co-adsorption effects[25, 49-50, 52].

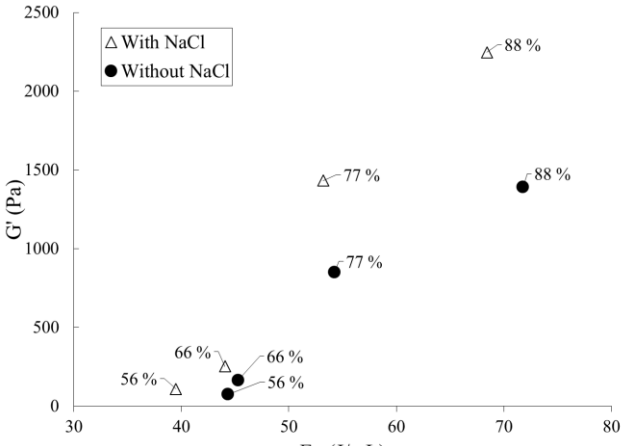

Figure 9. The elastic shear modulus as a function of the energy incorporated through the emulsification process for emulsions prepared with 0.5% wt of NaCl (empty symbols) and without NaCl (filled symbols) within the volume fraction range used in this work.

Interfacial shear rheology

Assessment of the mechanisms behind the stabilization effect of electrolytes such as NaCl mentioned in the previous sections is highly relevant because of its impact in the long-term physical stability of W/O emulsions. Interfacial shear rheology provides information at the molecular level in terms of the elasticity of the adsorbed layer. Fig. 10 shows a plot of the elastic interfacial shear modulus ($G^{s\prime}$) as a function of the volume fraction of the dispersed phase. The first observation is that $G^{s\prime}$ increases with volume fraction for emulsions without salt. This is an intuitive and expected result because as the amount of aqueous phase increases, the interfacial area increases and so the surfactants will cover it (given that the amount of surfactant used in this work is significantly above the *cmc*) generating strong and elastic multilayers. The second observation, which is interesting and counterintuitive is that $G^{s\prime}$ decreases with volume fraction for emulsions prepared with NaCl. And the third observation is that $G^{s\prime}$ for emulsions with salt is significantly lower in all cases than $G^{s\prime}$ for emulsions without electrolyte. To answer the question of why the interfacial elasticity of a

system that is clearly more stable to coarsening of droplets and consistently showed higher values of G', decreases, an analysis of the processes that take place at the liquid-liquid interface is required.

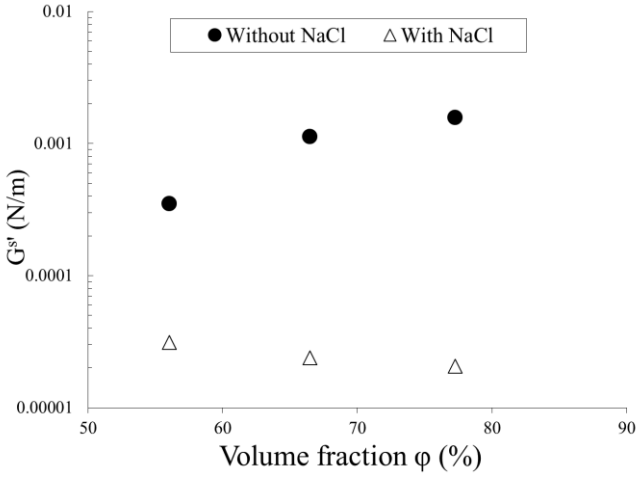

Figure 10. The elastic interfacial shear modulus as function of the volume fraction of the dispersed phase for emulsions without NaCl (filled symbols) and prepared with 0.5 %wt of NaCl (empty symbols). Note that the values of volume fraction reported are simply a way of naming the equivalent amounts in bulk phases of the actual emulsions prepared.

According to the Hofmeister series[63] anions can be classified in terms of polarity: $SO_4^{2-} > HPO_4^{2-} > F^- > Cl^- > Br^- > I^- (\cong ClOO_4^-) > SCN^-$. One line of thought states that those anions located to the left side of Cl^- (i.e. anions that elute first in a packed-column) are polar

kosmotropes or "structure makers" that stabilize non-electrolyte species by a salting-in effect. Similarly, those anions located to the right side of the series are considered structure breakers that tend to decrease the solubility of organic species by a salting-out effect. An alternative line of thought treats the slating in/out effects as a result of the adsorption/desorption of ions to the hydrophilic parts of the organic species (e.g. surfactant) causing a dehydration of the polar heads[50, 64]. This is what the results of Fig. 10 are showing and so the explanation of why $G^{s\prime}$ is lower and decreases with concentration for emulsions prepared with NaCl is given through a relaxation of the interface. When salt is added it interacts not only with the possible surface active impurities from the mineral oil but also with the polar heads of the surfactant mixture. Because NaCl can also adsorb (in fact it can lower the interfacial tension) at the liquid-liquid interface, it acts as a bridge between the polar heads and modifies the adsorption density relaxing the interface. The overall response of the system is then that E' is lower but in a coarsening event (e.g. Ostwald ripening, coalescence), this interface with salt will be more stable because surfactant migration at the interface will be more difficult. In this sense, NaCl has a salting-in effect due to co-adsorption and strong interactions at the W/O interface that generate bridging, a type of solvation, of the hydrophilic parts of the surfactants that ultimately relax the interface.

The implications of these results are impactful because a link between the response at the interfacial level and the processes that take place in bulk can be established. This link is not yet fully understood, which is the reason why multi-scale approaches must be used for further research on this topic.

CONCLUSIONS

Water-in-mineral oil emulsions with and without salt (NaCl) were prepared and a multiscale approach[42-43] was used to measure and evaluate their response at three different levels: macroscopic through G' (shear rheology), microscopic through average droplet size and droplet size distribution (LS and PFG-NMR) and molecular through $G^{s\prime}$ (interfacial shear rheology). Results at the microscopic and macroscopic level show that emulsions prepared with salt are consistently more rigid because of the higher bulk elasticity achieved ($G'_{with\ NaCl} > G'_{without\ NaCl}$). These results suggest that surfactant-stabilized emulsions with a moderate content of electrolyte would be more stable against coarsening through Ostwald ripening and coalescence because of interactions at the liquid-liquid interface and the preponderance of van der Waals interactions which is consistent with what has been reported in the literature[28, 52, 54, 57, 65].

PFG-NMR and LS results show that the microscopic properties of W/O emulsions without salt (droplet size and distribution) tend to increase and form a soft plateau after 20 days while these parameters for emulsions prepared with NaCl tend to remain constant. This means that the long-term physical stability follows a consistent behavior when salt is added to the system. The response is the same but more pronounced when the temperature is increased.

Emulsions prepared with salt required less energy to produce similar droplet sizes, distributions and higher values of G' within the volume fraction range evaluated. This is an interesting result because higher stabilization in the presence of salt is not due to changes in droplet size but instead to other processes that take place at the oil/water interface such as bridging (salting-in).

The processes and mechanisms that ultimately lead to a higher stability of W/O emulsions with salt was evaluated through interfacial shear rheology. Results show that when the salt dissociates it strongly interacts with the polar heads of the surfactant mixture and possibly with the surface active impurities from the mineral oil in a way that the interface relaxes because of a salting-in/bridging effect of the salt that changes the adsorption density of the layer. Hence contrary to the bulk-macroscopic response, the molecular response leads to $G^{s\prime}_{with\ NaCl} < G^{s\prime}_{without\ NaCl}$. This result shows that interfacial rheology can be used to infer the bulk response of these systems and that its influence is not necessarily straightforward which means that research on such link is needed.

ACKNOWLEDGEMENTS

The authors would like to give special thanks to Dr. Sébastien Simon (Ugelstad Laboratory, NTNU, Norway) for his valuable input and fruitful discussions during the writing of this article.

REFERENCES

1. Sjöblom, J., Stenius, Per., Simon Sébastien and Grimes, Brian., Emulsion Stabilization. In *Encyclopedia of Colloid and Interface Science*, Tadros, T., Ed. Springer: Berlin, 2013; Vol. 1-A-M, pp 415-454.
2. Pal, R., Rheology of high internal phase ratio emulsions. *Food Hydrocolloids* **2006,** *20*, 997-1005.
3. Dickinson, E.; Miller, R.; Chemistry, R. S. o., *Food Colloids: Fundamentals of Formulation*. Royal Society of Chemistry: 2001.
4. McClements, D. J., *Food Emulsions: Principles, Practices, and Techniques, Third Edition*. CRC Press: 2015.
5. Kilpatrick, P., Spiecker, P. , Asphaltene Emulsions In *Encyclopedic Handbook of Emulsion Technology*, J, S., Ed. Marcel Dekker: New York, 2001.
6. Kilpatrick, P. K., Water-in-Crude Oil Emulsion Stabilization: Review and Unanswered Questions. *Energy & Fuels* **2012,** *26* (7), 4017-4026.
7. Sjöblom, J.; Aske, N.; Auflem, I. H.; Brandal, Ø.; Havre, T. E.; Sæther, Ø.; Westvik, A.; Johnsen, E. E.; Kallevik, H., Our current understanding of water-in-crude oil emulsions.

Recent characterization techniques and high pressure performance. *Advances in Colloid and Interface Science* **2003,** *100-102* (SUPPL.), 399-473.
8. Leal-Calderon, F., Schmitt, V., Bibette, J., *Emulsion Science: Basic Principles.* . Springer: New York, 2007.
9. Verruto, V. J., Kilpatrick P., Water-in-Model Oil Emulsions Studied by Small-Angle Neutron Scattering: Interfacial Film Thickness and Composition. *Langmuir* **2008,** *24*, 12807-12822.
10. Masalova, I.; Foudazi, R.; Malkin, A. Y., The rheology of highly concentrated emulsions stabilized with different surfactants. *Colloids and Surfaces A: Physicochemical and Engineering Aspects* **2011,** *375* (1-3), 76-86.
11. Pal, R., Rheology of high internal phase ratio emulsions. *Food Hydrocolloids* **2006,** *20* (7), 997-1005.
12. Masalova, I.; Malkin, A. Y., Master curves for elastic and plastic properties of highly concentrated emulsions. *Colloid Journal* **2008,** *70* (3), 327-336.
13. Pal, R., Yield stress and viscoelastic properties of high internal phase ratio emulsions. *Colloid and Polymer Science* **1999,** *277* (6), 583-588.
14. Malkin, A. Y.; Masalova, I.; Slatter, P.; Wilson, K., Effect of droplet size on the rheological properties of highly-concentrated w/o emulsions. *Rheologica Acta* **2004,** *43* (6), 584-591.
15. Derkach, S. R., Rheology of emulsions. *Advances in Colloid and Interface Science* **2009,** *151* (1-2), 1-23.
16. Mason, T. G.; Lacasse, M. D.; Grest, G. S.; Levine, D.; Bibette, J.; Weitz, D. A., Osmotic pressure and viscoelastic shear moduli of concentrated emulsions. *Physical Review E - Statistical Physics, Plasmas, Fluids, and Related Interdisciplinary Topics* **1997,** *56* (3 B), 3150-3166.
17. Mougel, J.; Alvarez, O.; Baravian, C.; Caton, F.; Marchal, P.; Stébé, M. J.; Choplin, L., Aging of an unstable w/o gel emulsion with a nonionic surfactant. *Rheologica Acta* **2006,** *45* (5), 555-560.
18. Datta, S. S.; Gerrard, D. D.; Rhodes, T. S.; Mason, T. G.; Weitz, D. A., Rheology of attractive emulsions. *Physical Review E - Statistical, Nonlinear, and Soft Matter Physics* **2011,** *84* (4).
19. Tadros, T., Application of rheology for assessment and prediction of the long-term physical stability of emulsions. *Advances in Colloid and Interface Science* **2004,** *108-109*, 227-258.
20. Langevin, D., Influence of interfacial rheology on foam and emulsion properties. *Advances in Colloid and Interface Science* **2000,** *88* (1), 209-222.
21. Georgieva, D.; Schmitt, V.; Leal-Calderon, F.; Langevin, D., On the Possible Role of Surface Elasticity in Emulsion Stability. *Langmuir* **2009,** *25* (10), 5565-5573.
22. Kent, P.; Saunders, B. R., The Role of Added Electrolyte in the Stabilization of Inverse Emulsions. *Journal of Colloid and Interface Science* **2001,** *242* (2), 437-442.
23. Jiang, J.; Mei, Z.; Xu, J.; Sun, D., Effect of inorganic electrolytes on the formation and the stability of water-in-oil (W/O) emulsions. *Colloids and Surfaces A: Physicochemical and Engineering Aspects* **2013,** *429*, 82-90.
24. Albers, W.; Overbeek, J. T. G., Stability of emulsions of water in oil: II. Charge as a factor of stabilization against flocculation. *Journal of Colloid Science* **1959,** *14* (5), 510-518.

25. Aronson, M. P.; Petko, M. F., Highly Concentrated Water-in-Oil Emulsions: Influence of Electrolyte on Their Properties and Stability. *Journal of Colloid and Interface Science* **1993,** *159* (1), 134-149.
26. Griffin, W., Classification of Surface-Active Agents by "HLB". *Journal of Cosmetic Science* **1949,** *1* (5), 311-326.
27. Opawale, F. O.; Burgess, D. J., Influence of Interfacial Properties of Lipophilic Surfactants on Water-in-Oil Emulsion Stability. *Journal of Colloid and Interface Science* **1998,** *197* (1), 142-150.
28. Leal-Calderon, F.; Mondain-Monval, O.; Pays, K.; Royer, N.; Bibette, J., Water-in-Oil Emulsions: Role of the Solvent Molecular Size on Droplet Interactions. *Langmuir* **1997,** *13* (26), 7008-7011.
29. Shields, M.; Ellis, R.; Saunders, B. R., A creaming study of weakly flocculated and depletion flocculated oil-in-water emulsions. *Colloids and Surfaces A: Physicochemical and Engineering Aspects* **2001,** *178* (1), 265-276.
30. Koh, A.; Gillies, G.; Gore, J.; Saunders, B. R., Flocculation and Coalescence of Oil-in-Water Poly(dimethylsiloxane) Emulsions. *Journal of Colloid and Interface Science* **2000,** *227* (2), 390-397.
31. Clausse, D., Daniel-David, D., Gomez, F., Komunjer, L., Pezron, I., Dalmazzone, C., Noïk, C., 5. Emulsion Stability and Interfacial Properties – Application to Complex Emulsions of Industrial Interest. In *Colloid Stability and Application in Pharmacy*, Tadros, T. F., Ed. Wiley-VCH Verlag GmbH & Co. KGaA: Weinheim, Germany, 2007; Vol. 3.
32. Py, C.; Rouvière, J.; Loll, P.; Taelman, M. C.; Tadros, T. F., Investigation of multiple emulsion stability using rheological measurements. *Colloids and Surfaces A: Physicochemical and Engineering Aspects* **1994,** *91*, 215-225.
33. Salager, J.-L., Guidelines to handle the formulation, composition and stirring to attain emulsion properties on design (type, drop size, viscosity and stability). In *Surfactants in Solution in Surfactant Science Series*, 1996; Vol. 64, pp 261-295.
34. Keleşoğlu, S.; Barrabino Ponce, A.; Humborstad Sørland, G.; Simon, S.; Paso, K.; Sjöblom, J., Rheological properties of highly concentrated dense packed layer emulsions (w/o) stabilized by asphaltene. *Journal of Petroleum Science and Engineering* **2015,** *126*, 1-10.
35. Dukhin S, S., J., Saether, O, An Experimental and Theoretical Approach to the Dynamic Behavior of Emulsions. In *Emulsions and Emulsion Stability*, 2nd ed.; Sjöblom, J., Ed. CRC Press. Taylor and Francis Group: Boca Raton, FL, 2006.
36. Angle, C. W., Chemical Demulsification of Stable Crude Oil and Bitumen Emulsions in Petroleum Recovery-A Review. In *Encyclopedic Handbook of Emulsion Technology*, Sjöblom, J., Ed. Marcel Dekker: New York, 2001; pp 541-594.
37. Tanner, J. E.; Stejskal, E. O., Restricted Self-Diffusion of Protons in Colloidal Systems by the Pulsed-Gradient, Spin-Echo Method. *The Journal of Chemical Physics* **1968,** *49* (4), 1768-1777.
38. Le Doussal, P.; Sen, P. N., Nuclear magnetization relaxation by diffusion in a parabolic magnetic field. *Physica A: Statistical Mechanics and its Applications* **1992,** *186* (1), 115-120.
39. Mitra, P. P.; Sen, P. N., Effects of surface relaxation on NMR pulsed field gradient experiments in porous media. *Physica A: Statistical Mechanics and its Applications* **1992,** *186* (1), 109-114.

40. Sørland, G., *Dynamic Pulsed-Field-Gradient NMR*. Springer, Berlin, Heidelberg 2014.
41. Mitra, P. P.; Sen, P. N.; Schwartz, L. M., Short-time behavior of the diffusion coefficient as a geometrical probe of porous media. *Physical Review B* **1993,** *47* (14), 8565-8574.
42. Gallo-Molina, J. P.; Ratkovich, N.; Álvarez, Ó., Multiscale Analysis of Water-in-Oil Emulsions: A Computational Fluid Dynamics Approach. *Industrial and Engineering Chemistry Research* **2017,** *56* (27), 7757-7767.
43. Pradilla, D.; Vargas, W.; Alvarez, O., The application of a multi-scale approach to the manufacture of concentrated and highly concentrated emulsions. *Chemical Engineering Research and Design* **2015,** *95*, 162-172.
44. Marques, D. S.; Sørland, G.; Less, S.; Vilagines, R., The application of pulse field gradient (PFG) NMR methods to characterize the efficiency of separation of water-in-crude oil emulsions. *Journal of Colloid and Interface Science* **2018,** *512*, 361-368.
45. Vandebril, S.; Franck, A.; Fuller, G. G.; Moldenaers, P.; Vermant, J., A double wall-ring geometry for interfacial shear rheometry. *Rheologica Acta* **2010,** *49* (2), 131-144.
46. Sørland, G. H.; Aksnes, D.; Gjerdåker, L., A Pulsed Field Gradient Spin-Echo Method for Diffusion Measurements in the Presence of Internal Gradients. *Journal of Magnetic Resonance* **1999,** *137* (2), 397-401.
47. Dimitrova, T. D.; Leal-Calderon, F., Rheological properties of highly concentrated protein-stabilized emulsions. *Advances in Colloid and Interface Science* **2004,** *108-109*, 49-61.
48. Lacasse, M.-D.; Grest, G. S.; Levine, D.; Mason, T. G.; Weitz, D. A., Model for the Elasticity of Compressed Emulsions. *Physical Review Letters* **1996,** *76* (18), 3448-3451.
49. Kabalnov, A.; Weers, J., Macroemulsion Stability within the Winsor III Region: Theory versus Experiment. *Langmuir* **1996,** *12* (8), 1931-1935.
50. Iwanaga, T.; Suzuki, M.; Kunieda, H., Effect of Added Salts or Polyols on the Liquid Crystalline Structures of Polyoxyethylene-Type Nonionic Surfactants. *Langmuir* **1998,** *14* (20), 5775-5781.
51. Israelachvili, J., *Intermolecular and surface forces*. third ed.; Elsevier: San Diego; Oxford, 2011.
52. Márquez, A. L.; Medrano, A.; Panizzolo, L. A.; Wagner, J. R., Effect of calcium salts and surfactant concentration on the stability of water-in-oil (w/o) emulsions prepared with polyglycerol polyricinoleate. *Journal of Colloid and Interface Science* **2010,** *341* (1), 101-108.
53. Princen, H. M.; Kiss, A. D., Rheology of foams and highly concentrated emulsions: III. Static shear modulus. *Journal of Colloid and Interface Science* **1986,** *112* (2), 427-437.
54. Mougel, J.; Alvarez, O.; Baravian, C.; Caton, F.; Marchal, P.; Stébé, M.-J.; Choplin, L., Aging of an unstable w/o gel emulsion with a nonionic surfactant. *Rheologica Acta* **2006,** *45* (5), 555-560.
55. Mason, T. G.; Lacasse, M.-D.; Grest, G. S.; Levine, D.; Bibette, J.; Weitz, D. A., Osmotic pressure and viscoelastic shear moduli of concentrated emulsions. *Physical Review E* **1997,** *56* (3), 3150-3166.
56. Dukhin, S., Goetz, P, Ionic properties of so-called "non-ionic" surfactants in non-polar liquids. In *Dispersion Technology, Inc.*

57. Paruta-Tuarez, E.; Marchal, P.; Sadtler, V.; Choplin, L., Analysis of the Princen and Kiss Equation To Model the Storage Modulus of Highly Concentrated Emulsions. *Industrial & Engineering Chemistry Research* **2011,** *50* (17), 10359-10365.
58. Mason, T. G., New fundamental concepts in emulsion rheology. *Current Opinion in Colloid & Interface Science* **1999,** *4* (3), 231-238.
59. Weiss, J.; Canceliere, C.; McClements, D. J., Mass Transport Phenomena in Oil-in-Water Emulsions Containing Surfactant Micelles: Ostwald Ripening. *Langmuir* **2000,** *16* (17), 6833-6838.
60. Schmitt, V.; Cattelet, C.; Leal-Calderon, F., Coarsening of Alkane-in-Water Emulsions Stabilized by Nonionic Poly(oxyethylene) Surfactants: The Role of Molecular Permeation and Coalescence. *Langmuir* **2004,** *20* (1), 46-52.
61. Tcholakova, S.; Lesov, I.; Golemanov, K.; Denkov, N. D.; Judat, S.; Engel, R.; Danner, T., Efficient Emulsification of Viscous Oils at High Drop Volume Fraction. *Langmuir* **2011,** *27* (24), 14783-14796.
62. Tcholakova, S.; Denkov, N. D.; Sidzhakova, D.; Ivanov, I. B.; Campbell, B., Effects of Electrolyte Concentration and pH on the Coalescence Stability of β-Lactoglobulin Emulsions: Experiment and Interpretation. *Langmuir* **2005,** *21* (11), 4842-4855.
63. Collins, K. D.; Washabaugh, M. W., The Hofmeister effect and the behaviour of water at interfaces. *Quarterly Reviews of Biophysics* **2009,** *18* (4), 323-422.
64. Alexandridis, P.; Holzwarth, J. F., Differential Scanning Calorimetry Investigation of the Effect of Salts on Aqueous Solution Properties of an Amphiphilic Block Copolymer (Poloxamer). *Langmuir* **1997,** *13* (23), 6074-6082.
65. Dimitrova, T., Leal-Calderon, F. , Bulk elasticity of concentrated protein-stabilized emulsions. *Langmuir* **2001,** *17*, 3235-3244.